

# Argmax Flows and Multinomial Diffusion: Towards Non-Autoregressive Language Models

Emiel Hoogeboom<sup>\*1</sup> Didrik Nielsen<sup>\*2</sup> Priyank Jaini<sup>1</sup> Patrick Forré<sup>3</sup> Max Welling<sup>1</sup>

## Abstract

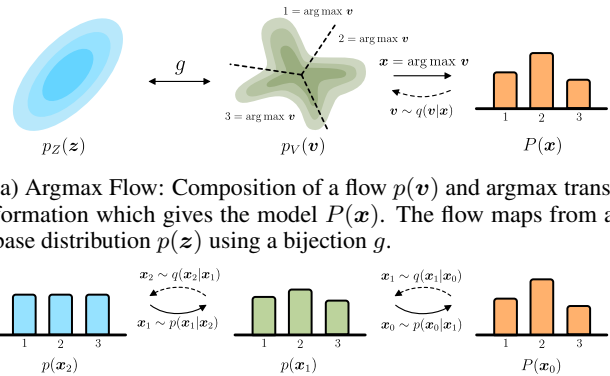
The field of language modelling has been largely dominated by autoregressive models, for which sampling is inherently difficult to parallelize. This paper introduces two new classes of generative models for categorical data such as language or image segmentation: *Argmax Flows* and *Multinomial Diffusion*. Argmax Flows are defined by a composition of a continuous distribution (such as a normalizing flow), and an argmax function. To optimize this model, we learn a probabilistic inverse for the argmax that lifts the categorical data to a continuous space. Multinomial Diffusion gradually adds categorical noise in a diffusion process, for which the generative denoising process is learned. We demonstrate that our models perform competitively on language modelling and modelling of image segmentation maps.

## 1. Introduction

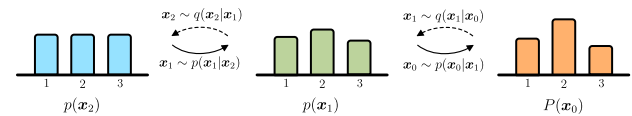
Many sources of high-dimensional data are categorical, for example language and image segmentation. Although natural images with ordinal representations have been studied to a large extent with generative models such as normalizing flows or recently diffusion models, categorical data has not had the same extensive treatment and is currently primarily modelled by autoregressive models (Cooijmans et al., 2017; Al-Rfou et al., 2019; Dai et al., 2019; Child et al., 2019).

Normalizing flows are attractive because they can be designed to be fast both in the inference and sampling direction, for instance using coupling layers (Dinh et al., 2015). Typically, normalizing flows model continuous distributions. As a result, directly optimizing a flow on discrete data may lead to arbitrarily high likelihoods. In literature this problem is resolved for ordinal data by adding noise in a unit interval

<sup>1</sup>UvA-Bosch Delta Lab, University of Amsterdam <sup>2</sup>Technical University of Denmark <sup>3</sup>University of Amsterdam, Netherlands. Correspondence to: Emiel Hoogeboom <e.hoogeboom@uva.nl>, Didrik Nielsen <didni@dtu.dk>.



(a) Argmax Flow: Composition of a flow  $p(\mathbf{v})$  and argmax transformation which gives the model  $P(\mathbf{x})$ . The flow maps from a base distribution  $p(\mathbf{z})$  using a bijection  $g$ .



(b) Multinomial Diffusion: Each step  $p(\mathbf{x}_{t-1}|\mathbf{x}_t)$  denoises the signal starting from a uniform categorical base distribution which gives the model  $P(\mathbf{x}_0)$ .

Figure 1. Overview of Argmax Flows and Multinomial Diffusion.

around the discrete value (Uria et al., 2013; Theis et al., 2016; Ho et al., 2019). However, because these methods have been designed for ordinal data, directly applying dequantization to categorical data leads to sub-optimal results.

An alternative class of likelihood based generative models are Diffusion models (Sohl-Dickstein et al., 2015), which are fast to train due to an objective that decomposes over time steps (Ho et al., 2020). Diffusion models generally have a fixed diffusion process that gradually adds noise. This process is complemented by a learnable generative process, that essentially denoises the signal. Although diffusion models for continuous and binary variables have been proposed, an approach for categorical variables is not yet known. Although in theory diffusion models require many steps to generate a sample, recent methods (Song et al., 2020a; Nichol & Dhariwal, 2021) show that in practice the number of steps can be significantly reduced for sampling.

In this paper we introduce two new generative models for categorical variables (depicted in Figure 1): *i*) Argmax Flows bridge the gap between categorical data and continuous normalizing flows using an argmax transformation and a corresponding family of probabilistic inverses for the argmax. *ii*) Multinomial Diffusion provides a diffusion framework for categorical variables based on categorical transition distributions.

Table 1. Surjective flow layers for applying continuous flow models to discrete data. The layers are deterministic in the generative direction, but stochastic in the inference direction. Rounding corresponds to the commonly-used dequantization for ordinal data.

Layer	Generation	Inference	Applications
Rounding	$\mathbf{x} = \lfloor \mathbf{v} \rfloor$	$\mathbf{v} \sim q(\mathbf{v} \mathbf{x})$ with support $\mathcal{S}(\mathbf{x}) = \{\mathbf{v} \mathbf{x} = \lfloor \mathbf{v} \rfloor\}$	Ordinal Data e.g. images, audio
Argmax	$\mathbf{x} = \arg \max \mathbf{v}$	$\mathbf{v} \sim q(\mathbf{v} \mathbf{x})$ with support $\mathcal{S}(\mathbf{x}) = \{\mathbf{v} \mathbf{x} = \arg \max \mathbf{v}\}$	Categorical Data e.g. text, segmentation

## 2. Background

This section introduces first introduces normalizing flows and the change-of-variables formula. Secondly diffusion models and their optimization procedure are explained.

### 2.1. Normalizing Flows

Given  $\mathcal{V} = \mathbb{R}^d$  and  $\mathcal{Z} = \mathbb{R}^d$  with densities  $p_V$  and  $p_Z$  respectively, normalizing flows (Rezende & Mohamed, 2015) learn a bijective and differentiable transformation  $g: \mathcal{Z} \rightarrow \mathcal{V}$  such that the change-of-variables formula gives the density at any point  $\mathbf{v} \in \mathcal{V}$ :

$$p_V(\mathbf{v}) = p_Z(\mathbf{z}) \cdot \left| \det \frac{d\mathbf{z}}{d\mathbf{v}} \right|, \quad \mathbf{v} = g(\mathbf{z}), \quad (1)$$

where  $p_Z$  can be any density (usually chosen as a standard Gaussian). Thus, normalizing flows provide a powerful framework to learn *exact* density functions. However, Equation (1) is restricted to continuous densities.

Uria et al. (2013) proposed to model  $p(\mathbf{v})$  for integer data  $\mathbf{x}$  using  $\mathbf{v} = \mathbf{x} + \mathbf{u}$  where  $\mathbf{u} \sim \mathcal{U}(0, 1)^d$ . Theis et al. (2016) showed that  $\log p(\mathbf{v})$  lower bounds an implied discrete distribution  $P(\mathbf{x})$ . Ho et al. (2019) extended this framework for variational distributions  $q(\mathbf{u}|\mathbf{x})$ . Hooeboom et al. (2020) showed that from a latent variable perspective, not only hypercubes, but any partitioning of the space  $\mathcal{V}$  can be optimized using this objective. Further, Nielsen et al. (2020) reinterpreted dequantization as a surjective flow layer  $\mathbf{v} \mapsto \mathbf{x}$  that is deterministic in one direction (since  $\mathbf{x} = \text{round}(\mathbf{v})$ ) and stochastic in the other ( $\mathbf{v} = \mathbf{x} + \mathbf{u}$  where  $\mathbf{u} \sim q(\mathbf{u}|\mathbf{x})$ ). Using this interpretation, dequantization can be seen as a probabilistic right-inverse for the rounding operation in the latent variable model given by:

$$P(\mathbf{x}) = \int P(\mathbf{x}|\mathbf{v})p(\mathbf{v}) d\mathbf{v}, \quad P(\mathbf{x}|\mathbf{v}) = \delta(\mathbf{x} = \text{round}(\mathbf{v})),$$

where  $\text{round}$  is applied elementwise. In this case, the density model  $p(\mathbf{v})$  is modeled using a normalizing flow. Learning proceeds by introducing the variational distribution  $q(\mathbf{v}|\mathbf{x})$  that models the probabilistic right-inverse for the rounding surjection and optimizing the evidence lower bound (ELBO):

$$\begin{aligned} \log P(\mathbf{x}) &\geq \mathbb{E}_{\mathbf{v} \sim q(\mathbf{v}|\mathbf{x})} [\log P(\mathbf{x}|\mathbf{v}) + \log p(\mathbf{v}) - \log q(\mathbf{v}|\mathbf{x})] \\ &= \mathbb{E}_{\mathbf{v} \sim q(\mathbf{v}|\mathbf{x})} [\log p(\mathbf{v}) - \log q(\mathbf{v}|\mathbf{x})]. \end{aligned} \quad (2)$$

The last equality holds under the constraint that the support of  $q(\mathbf{v}|\mathbf{x})$  is enforced to be only over the region  $\mathcal{S} = \{\mathbf{v} \in \mathbb{R}^d : \mathbf{x} = \text{round}(\mathbf{v})\}$  which ensures that  $P(\mathbf{x}|\mathbf{v}) = 1$ .

### 2.2. Diffusion Models

Let the data variable be denoted by  $\mathbf{x}_0$ . A diffusion chain (Sohl-Dickstein et al., 2015) consists of predefined variational distributions  $q(\mathbf{x}_t|\mathbf{x}_{t-1})$  that gradually add noise over time steps. The joint distribution of  $q(\mathbf{x}_t|\mathbf{x}_{t-1})$  for a large number of timesteps  $T$  is referred to in literature as the forward (or *diffusion*) trajectory:

$$q(\mathbf{x}_1, \dots, \mathbf{x}_T|\mathbf{x}_0) = \prod_{t=1}^T q(\mathbf{x}_t|\mathbf{x}_{t-1}). \quad (3)$$

The diffusion trajectory is typically defined such that  $q(\mathbf{x}_t|\mathbf{x}_{t-1})$  adds a small amount of noise around  $\mathbf{x}_{t-1}$ . This way, information is gradually destroyed such that at the final time step,  $\mathbf{x}_T$  carries almost no information about  $\mathbf{x}_0$ . There are generally only little or even no learnable parameters in  $q$ . The generative counterpart to the diffusion process is described by learnable distributions  $p(\mathbf{x}_{t-1}|\mathbf{x}_t)$  that define the reverse (or *denoising*) trajectory:

$$p(\mathbf{x}_T, \dots, \mathbf{x}_0) = p(\mathbf{x}_T) \prod_{t=1}^T p(\mathbf{x}_{t-1}|\mathbf{x}_t), \quad (4)$$

When the diffusion process adds sufficiently small amounts of noise, it suffices to define the denoising trajectory using distributions that are factorized (without correlation) over the dimension axis. The distribution  $p(\mathbf{x}_T)$  is chosen to be similar to the distribution that the diffusion trajectory approaches.

Sohl-Dickstein et al. (2015) defined two specific diffusion models: 1) For *Gaussian diffusion*,  $q(\mathbf{x}_t|\mathbf{x}_{t-1}) = \mathcal{N}(\sqrt{1 - \beta_t}\mathbf{x}_{t-1}, \beta_t I)$  and  $p(\mathbf{x}_T) = \mathcal{N}(0, I)$ , where the diffusion parameters  $\{\beta_t\}$  can be fixed beforehand. 2) *Binomial Diffusion* diffuses multivariate Bernoulli distributions using a forward trajectory and a learnable reverse trajectory using a function approximator such as neural networks to predict the Bernoulli parameters  $\mu_t$ :

$$q(\mathbf{x}_t|\mathbf{x}_{t-1}) = \mathcal{B}(\mathbf{x}_t|(1 - \beta_t)\mathbf{x}_{t-1} + 0.5\beta_t) \quad (5)$$

$$p(\mathbf{x}_{t-1}|\mathbf{x}_t) = \mathcal{B}(\mathbf{x}_{t-1}|\mu_t(\mathbf{x}_t)) \quad (6)$$

**Optimization** The lower bound on the log-probability of the latent variable model  $P(\mathbf{x}_0) = \int_{\mathbf{x}_1, \dots, \mathbf{x}_T} p(\mathbf{x}_T, \dots, \mathbf{x}_0)$

---

**Algorithm 1** Sampling from Argmax Flows

---

**Input:**  $p(\mathbf{v})$   
**Output:** Sample  $\mathbf{x}$   
 Sample  $\mathbf{v} \sim p(\mathbf{v})$   
 Compute  $\mathbf{x} = \arg \max \mathbf{v}$

---

can be derived with variational inference as follows:

$$\log P(\mathbf{x}_0) \geq \mathbb{E}_{\mathbf{x}_1, \dots, \mathbf{x}_T \sim q} \left[ \log p(\mathbf{x}_T) + \sum_{t=1}^T \log \frac{p(\mathbf{x}_{t-1}|\mathbf{x}_t)}{q(\mathbf{x}_t|\mathbf{x}_{t-1})} \right].$$

An important insight in diffusion is that by conditioning on  $\mathbf{x}_0$ , the posterior probability (Sohl-Dickstein et al., 2015):

$$q(\mathbf{x}_{t-1}|\mathbf{x}_t, \mathbf{x}_0) = \frac{q(\mathbf{x}_t|\mathbf{x}_{t-1})q(\mathbf{x}_{t-1}|\mathbf{x}_0)}{q(\mathbf{x}_t|\mathbf{x}_0)}, \quad (7)$$

can be computed directly when  $q$  is a simple distribution such as a Gaussian or Bernoulli and the process is Markov. This permits a reformulation of the lower bound using KL divergences as follows, which will have much lower variance during optimization:

$$\begin{aligned} \log P(\mathbf{x}_0) &\geq \mathbb{E}_{\mathbf{x}_1, \dots, \mathbf{x}_T \sim q} \left[ -\text{KL}(q(\mathbf{x}_T|\mathbf{x}_0)|p(\mathbf{x}_T)) + \right. \\ &\left. \log p(\mathbf{x}_0|\mathbf{x}_1) - \sum_{t=2}^T \text{KL}(q(\mathbf{x}_{t-1}|\mathbf{x}_t, \mathbf{x}_0)|p(\mathbf{x}_{t-1}|\mathbf{x}_t)) \right]. \end{aligned} \quad (8)$$

This equation can be rewritten to aid readability. By defining loss components  $L_0 = -\log p(\mathbf{x}_0|\mathbf{x}_1)$  and  $L_{t-1} = \text{KL}(q(\mathbf{x}_{t-1}|\mathbf{x}_t, \mathbf{x}_0)|p(\mathbf{x}_{t-1}|\mathbf{x}_t))$  for  $t \geq 2$ . Then the lowerbound is:

$$\log P(\mathbf{x}_0) \geq \mathbb{E}_{\mathbf{x}_1, \dots, \mathbf{x}_T \sim q} \left[ -\sum_{t=0}^{T-1} L_t - \underbrace{\text{KL}(q(\mathbf{x}_T|\mathbf{x}_0)|p(\mathbf{x}_T))}_{\approx 0} \right], \quad (9)$$

where  $\text{KL}(q(\mathbf{x}_T|\mathbf{x}_0)|p(\mathbf{x}_T)) \approx 0$  if the diffusion trajectory  $q$  is defined well. To significantly speed-up training, a timestep  $t$  for each batch element is sampled, and only  $L_t$  is optimized for that specific element.

### 3. Argmax Flows

Argmax flows define discrete distributions using 1) a density model  $p(\mathbf{v})$ , such as a normalizing flow, and 2) an argmax layer that maps the continuous  $\mathbf{v} \in \mathbb{R}^{D \times K}$  to a discrete  $\mathbf{x} \in \{1, 2, \dots, K\}^D$  using

$$\mathbf{x} = \arg \max \mathbf{v} \quad \text{where} \quad x_d = \arg \max_k v_{dk}. \quad (10)$$

Sampling from this model is straightforward, as shown in Alg. 1. To generate reasonable samples, it is up to the density model  $p(\mathbf{v})$  to capture any complicated dependencies between the different dimensions.

While sampling from an argmax flow is straightforward, the main difficulty lies in *optimizing* this generative model. To

---

**Algorithm 2** Optimizing Argmax Flows

---

**Input:**  $\mathbf{x}, p(\mathbf{v}), q(\mathbf{v}|\mathbf{x})$   
**Output:** ELBO  $\mathcal{L}$   
 Sample  $\mathbf{v} \sim q(\mathbf{v}|\mathbf{x})$   
 Compute  $\mathcal{L} = \log p(\mathbf{v}) - \log q(\mathbf{v}|\mathbf{x})$

---

compute the likelihood of a datapoint  $\mathbf{x}$ , we have to compute

$$P(\mathbf{x}) = \int P(\mathbf{x}|\mathbf{v})p(\mathbf{v})d\mathbf{v}, \quad P(\mathbf{x}|\mathbf{v}) = \delta(\mathbf{x} = \arg \max(\mathbf{v})), \quad (11)$$

which is intractable. Consequently, we resort to variational inference and specify a variational distribution  $q(\mathbf{v}|\mathbf{x})$ . We note that naively choosing any variational distribution may lead to samples  $\mathbf{v} \sim q(\mathbf{v}|\mathbf{x})$  where  $\delta(\mathbf{x} = \arg \max \mathbf{v}) = 0$ , which yields an ELBO of negative infinity. To avoid this, we need a variational distribution  $q(\mathbf{v}|\mathbf{x})$  that satisfies what we term the *argmax constraint*:

$$\mathbf{x} = \arg \max \mathbf{v} \quad \text{for all} \quad \mathbf{v} \sim q(\mathbf{v}|\mathbf{x}).$$

That is, the variational distribution  $q(\mathbf{v}|\mathbf{x})$  should have support limited to  $\mathcal{S}(\mathbf{x}) = \{\mathbf{v} \in \mathbb{R}^{D \times K} : \mathbf{x} = \arg \max \mathbf{v}\}$ . Recall that under this condition, the ELBO can be simplified as in Equation 2, as shown in Alg. 2. For an illustration of the method see Figure 1a.

#### 3.1. Probabilistic Inverse

The argmax layer may be viewed as a surjective flow layer (Nielsen et al., 2020). With this view, the variational distribution  $q(\mathbf{v}|\mathbf{x})$  specifies a distribution over the possible right-inverses of the argmax function, also known as a *stochastic inverse* or *probabilistic inverse*. Recall that the commonly-used dequantization layer for ordinal data corresponds to the probabilistic inverse of a rounding operation. As summarized in Table 1, this layer may thus be viewed as analogous to the argmax layer, where the round is for ordinal data while the argmax is for categorical data.

We are free to specify any variational distribution  $q(\mathbf{v}|\mathbf{x})$  that satisfies the argmax constraint. In the next paragraphs we outline three possible approaches. Since operations are performed independently across dimensions, we omit the dimension axis and let  $\mathbf{v} \in \mathbb{R}^K$  and  $x \in \{1, \dots, K\}$ .

**Thresholding (Alg. 3).** A relatively straightforward method to construct a distribution  $q(\mathbf{v}|\mathbf{x})$  satisfying the argmax constraint is to use thresholding. That is, we first sample an unbounded variable  $\mathbf{u} \in \mathbb{R}^K$  from  $q(\mathbf{u}|\mathbf{x})$ , which can be for example a conditional Gaussian or normalizing flow. Next, we map  $\mathbf{u}$  to  $\mathbf{v}$  such that element  $x$  is the largest:

$$v_x = u_x \quad \text{and} \quad \mathbf{v}_{-x} = \text{threshold}(\mathbf{u}_{-x}, T) \quad (12)$$

where the thresholding is applied elementwise with threshold value  $T = v_x$ . This ensures that element  $v_x$  is the

**Algorithm 3** Thresholding-based  $q(\mathbf{v}|\mathbf{x})$ 

**Input:**  $\mathbf{x}, q(\mathbf{u}|\mathbf{x})$   
**Output:**  $\mathbf{v}, \log q(\mathbf{v}|\mathbf{x})$   
 $\mathbf{u} \sim q(\mathbf{u}|\mathbf{x})$   
 $\mathbf{v}_x = \mathbf{u}_x$   
 $\mathbf{v}_{-x} = \text{threshold}(\mathbf{u}_{-x}, \mathbf{x})$   
 $\log q(\mathbf{v}|\mathbf{x}) = \log q(\mathbf{u}|\mathbf{x}) - \log |\det d\mathbf{v}/d\mathbf{u}|$

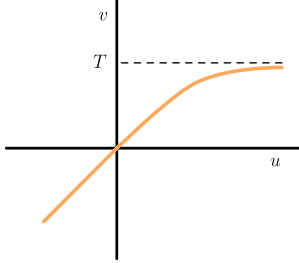


Figure 2. Visualization of the map  $v = \text{threshold}(u, T)$  that is used to ensure that outputs  $v < T$ .

largest, and consequently that  $q(\mathbf{v}|\mathbf{x})$  satisfies the argmax constraint.

Note that we require the threshold function to be bijective,  $\text{threshold} : \mathbb{R} \rightarrow (-\infty, T)$ , so that we can use the change-of-variables formula to compute  $\log q(\mathbf{v}|\mathbf{x})$ . In our implementation, thresholding is implemented using a softplus such that all values are mapped below a limit  $T$ :

$$v = \text{threshold}(u, T) = T - \text{softplus}(T - u), \quad (13)$$

where  $\text{softplus}(z) = \log(1 + e^z)$  and for which it is guaranteed that  $v \in (-\infty, T)$ , see Figure 2 for a visualization.

**Gumbel (Alg. 4).** An alternative approach is to let  $q(\mathbf{v}|\mathbf{x}) = \text{Gumbel}(\mathbf{v}|\phi)$  restricted to  $\arg \max \mathbf{v} = \mathbf{x}$ , where the location parameters  $\phi \leftarrow \text{NN}(\mathbf{x})$  are predicted using a neural network NN. The Gumbel distribution has favourable properties: The arg max and max are independent and the max is also distributed as a Gumbel:

$$\max_i v_i \sim \text{Gumbel}(\phi_{\max}), \quad (14)$$

where  $\phi_{\max} = \log \sum_i \exp \phi_i$ . For a more extensive introduction see (Maddison et al., 2014; Kool et al., 2019).

To sample  $\mathbf{v} \sim q(\mathbf{v}|\mathbf{x})$ , we thus first sample the maximum  $v_x$  according to Eq. 14. Next, given the sample  $v_x$ , the remaining values can be sampled using *truncated* Gumbel distributions:

$$v_i \sim \text{TruncGumbel}(\phi_i; T) \text{ where } i \neq x \quad (15)$$

where the truncation value  $T$  is given by  $v_x$  which ensures that the argmax constraint  $v_x > v_i$  for  $i \neq x$  is satisfied.

**Algorithm 4** Gumbel-based  $q(\mathbf{v}|\mathbf{x})$ 

**Input:**  $\mathbf{x}, \phi$   
**Output:**  $\mathbf{v}, \log q(\mathbf{v}|\mathbf{x})$   
 $\phi_{\max} = \log \sum_i \exp \phi_i$   
 $\mathbf{v}_x \sim \text{Gumbel}(\phi_{\max})$   
 $\mathbf{v}_{-x} \sim \text{TruncGumbel}(\phi_{-x}, \mathbf{v}_x)$   
 $\log q(\mathbf{v}|\mathbf{x}) = \log \text{Gumbel}(\mathbf{v}_x|\phi_{\max})$   
 $\quad + \log \text{TruncGumbel}(\mathbf{v}_{-x}|\phi_{-x}, \mathbf{v}_x)$

Recall that to optimize Eq. 2,  $\log q(\mathbf{v}|\mathbf{x})$  is also required, which can be computed using the closed-form expressions for the log density functions (see Table 2). Another property of Gumbel distributions is that

$$P(\arg \max \mathbf{v} = i) = \exp \phi_i / \sum_i \exp \phi_i, \quad (16)$$

which we use to initialize the location parameters  $\phi$  to match the empirical distribution of the first minibatch of the data.

**Gumbel Thresholding.** This method unifies the methods from the previous two sections: Gumbel distributions and thresholding. The key insight is that the Gumbel sampling procedures as defined above can be seen as a reparametrization of a uniform noise distribution  $\mathcal{U}(0, 1)^K$  which is put through the inverse CDF of the Gumbel distributions (see Table 2). From the perspective of change-of-variables, the log likelihood denotes the log volume change of this transformation. To increase expressivity the uniform distribution can be replaced by a normalizing flow  $q(\mathbf{u}|\mathbf{x})$  that has support on the interval  $(0, 1)^K$ , which can be enforced using a sigmoid transformation.

### 3.2. Cartesian Products of Argmax Flows

In the current description, Argmax Flows require the same number of dimensions in  $\mathbf{v}$  as there are classes in  $\mathbf{x}$ . To alleviate this constraint we introduce Cartesian products of Argmax Flows. To illustrate our method, consider a 256 class problem. One class can be represented using a single number in  $\{1, \dots, 256\}$ , but also using two hexadecimal numbers  $\{1, \dots, 16\}^2$  or alternatively using eight binary numbers. Specifically, any base  $K$  variable  $\mathbf{x}^{(K)} \in \{1, \dots, K\}^D$  can be converted to a base  $M$  variable  $\mathbf{x}^{(M)} \in \{1, \dots, M\}^{d_m \times D}$  where  $d_m = \lceil \log_M K \rceil$ .

Table 2. Summary of Gumbel properties.

Description	$\log p$	Sample
Gumbel( $g \phi$ )	$\phi - g - \exp(\phi - g)$	$g = -\log(-\log(u)) + \phi$ $u \sim \mathcal{U}(0, 1)$
$\max_i \text{Gumbel}(g_i \phi)$	$\log \text{Gumbel}(g_{\max} \phi_{\max})$ $\phi_{\max} = \log \sum_i \exp \phi_i$	$g_{\max} \sim \text{Gumbel}(\phi_{\max})$ $\phi_{\max} = \log \sum_i \exp \phi_i$
TruncGumbel( $g \phi, T$ )	$\phi - g - \exp(\phi - g) + \exp(\phi - T)$ if $g < T$ else $-\infty$	$g = \phi - \log(\exp(\phi - T) - \log u)$ $u \sim \mathcal{U}(0, 1)$

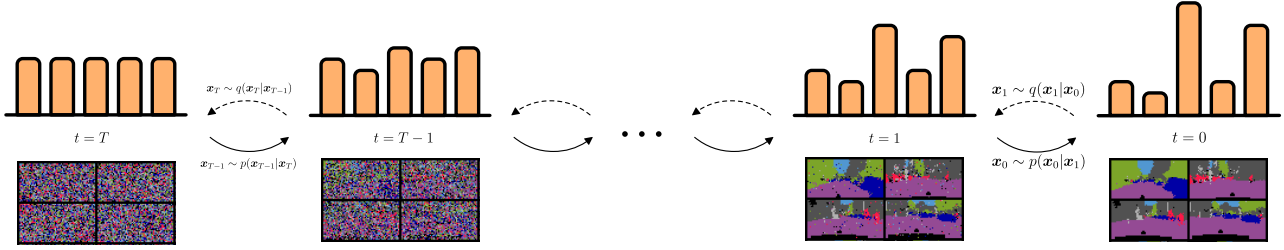


Figure 3. Overview of multinomial diffusion. A generative model  $p(\mathbf{x}_{t-1}|\mathbf{x}_t)$  learns to gradually denoise a signal from left to right. An inference diffusion process  $q(\mathbf{x}_t|\mathbf{x}_{t-1})$  gradually adds noise form right to left.

Table 3. Example of the trade-offs for Cartesian products of Argmax Flows, in a hypothetical problem with  $K = 2000$  classes.

$M$	$d_m$	neighbours	max distance	latent dimensions
2000	1	1999	1	2000
45	2	45	2	90
13	3	13	3	39
2	11	2	11	22

Then the variable  $\mathbf{x}^{(M)}$  with dimensionality  $M \cdot d_m \cdot D$  represents the variable  $\mathbf{x}^{(K)}$  with dimensionality  $K \cdot D$ , trading off symmetry for dimensionality. Even though this may lead to some unused additional classes, the ELBO objective in Equation 2 can still be optimized using an  $M$ -categorical Argmax Flow. To illustrate the changes in dimensionality, the properties of a hypothetical 2000-class problem is presented in Table 3. Finally, note that Cartesian products of binary spaces are a special case where the variable can be encoded symmetrically into a single dimension to the positive and negative part using binary dequantization (Winkler et al., 2019).

#### 4. Multinomial Diffusion

In this section we introduce an alternative likelihood-based model for categorical data: Multinomial Diffusion. In contrast with previous sections,  $\mathbf{x}_t$  will be represented in one-hot encoded format  $\mathbf{x}_t \in \{0, 1\}^K$ . Specifically, for category  $k$ ,  $x_k = 1$  and  $x_j = 0$  for  $j \neq k$ . Note that again the dimension axis is omitted for clarity as all distributions are independent over the dimension axis. We define the multinomial diffusion process using a categorical distribution that has a  $\beta_t$  chance of resampling a category uniformly:

$$q(\mathbf{x}_t|\mathbf{x}_{t-1}) = \mathcal{C}(\mathbf{x}_t|(1 - \beta_t)\mathbf{x}_{t-1} + \beta_t/K) \quad (17)$$

Since these distributions form a Markov chain, we can express the probability of any  $\mathbf{x}_t$  given  $\mathbf{x}_0$  as:

$$q(\mathbf{x}_t|\mathbf{x}_0) = \mathcal{C}(\mathbf{x}_t|\bar{\alpha}_t\mathbf{x}_0 + (1 - \bar{\alpha}_t)/K) \quad (18)$$

where  $\alpha_t = 1 - \beta_t$  and  $\bar{\alpha}_t = \prod_{\tau=1}^t \alpha_\tau$ .

Intuitively, for each next timestep, a little amount of uniform noise  $\beta_t$  over the  $K$  classes is introduced, and with a large probability  $(1 - \beta_t)$  the previous value  $\mathbf{x}_{t-1}$  is sampled.

Using Equation 17 and 18 the categorical posterior  $q(\mathbf{x}_{t-1}|\mathbf{x}_t, \mathbf{x}_0)$  can be directly computed. Although the exact expression is somewhat tedious to write out, the algorithmic steps to compute the probability vector are straightforward as shown in Algorithm 5 which we name  $\theta_{\text{posterior}}$ , where  $\odot$  denotes an elementwise multiplication and thus:

$$q(\mathbf{x}_{t-1}|\mathbf{x}_t, \mathbf{x}_0) = \mathcal{C}(\mathbf{x}_{t-1}|\theta_{\text{posterior}}(\mathbf{x}_t, \mathbf{x}_0)) \quad (19)$$

One of the innovations in (Ho et al., 2020) was the insight to not predict the parameters for the generative trajectory directly, but rather to predict the noise using the posterior equation for  $q$ . Although predicting the noise is difficult for discrete data, we propose to predict a probability vector for  $\hat{\mathbf{x}}_0$  from  $\mathbf{x}_t$  and subsequently parametrize  $p(\mathbf{x}_{t-1}|\mathbf{x}_t)$  using the probability vector from  $q(\mathbf{x}_{t-1}|\mathbf{x}_t, \hat{\mathbf{x}}_0)$ , where  $\mathbf{x}_0$  is approximated using a neural network  $\hat{\mathbf{x}}_0 = \mu(\mathbf{x}_t, t)$ . Algorithm 5 will produce valid probability vectors that are non-negative and sums to one under the condition that the prediction  $\hat{\mathbf{x}}_0$  is non-negative and sums to one, which is ensured with a softmax function in  $\mu$ . To summarize:

$$\begin{aligned} p(\mathbf{x}_0|\mathbf{x}_1) &= \mathcal{C}(\mathbf{x}_0|\hat{\mathbf{x}}_0) \\ p(\mathbf{x}_{t-1}|\mathbf{x}_t) &= \mathcal{C}(\mathbf{x}_{t-1}|\theta_{\text{posterior}}(\mathbf{x}_t, \hat{\mathbf{x}}_0)) \quad (20) \\ \text{where } \hat{\mathbf{x}}_0 &= \mu(\mathbf{x}_t, t) \end{aligned}$$

The KL terms in Equation 8 can be simply computed by enumerating the probabilities in Equation 19 and 20 and computing the KL divergence for discrete distributions in  $L_{t-1}$  with  $t \geq 2$ :

$$\begin{aligned} L_{t-1} &= \text{KL}(\mathcal{C}(\theta_{\text{posterior}}(\mathbf{x}_t, \mathbf{x}_0))|\mathcal{C}(\theta_{\text{posterior}}(\mathbf{x}_t, \hat{\mathbf{x}}_0))) \\ &= \sum_k \theta_{\text{posterior}}(\mathbf{x}_t, \mathbf{x}_0)_k \cdot \log \frac{\theta_{\text{posterior}}(\mathbf{x}_t, \mathbf{x}_0)_k}{\theta_{\text{posterior}}(\mathbf{x}_t, \hat{\mathbf{x}}_0)_k}, \quad (21) \end{aligned}$$

and to compute  $L_0 = -\log p(\mathbf{x}_0|\mathbf{x}_1)$  use that  $\mathbf{x}_0$  is onehot:

$$L_0 = -\sum_k \mathbf{x}_{0,k} \log \hat{\mathbf{x}}_{0,k} \quad (22)$$

---

**Algorithm 5**  $\theta_{\text{posterior}}(\mathbf{x}_t, \mathbf{x}_0)$

---

**Input:**  $\mathbf{x}_t, \mathbf{x}_0$

**Output:**  $\theta$

$$\theta_{\text{unnorm}} = [\mathbf{x}_t \alpha_t + (1 - \alpha_t)/K] \odot [\mathbf{x}_0 \bar{\alpha}_{t-1} + (1 - \bar{\alpha}_{t-1})/K]$$

$$\theta = \theta_{\text{unnorm}} / \sum_k \theta_{\text{unnorm},k}$$


---

Throughout this section we have assumed a single dimensional  $K$  class problem. Note that all equations translate to the multi-dimensional case independently, with as only exception the neural network  $\mu$ . This network predicts  $\hat{x}_0$  using dependence over all dimensions. For a numerically stable implementation in pseudo-code see Appendix A.

## 5. Related Work

Deep generative models broadly fall into the categories autoregressive models ARMs (Germain et al., 2015), Variational Autoencoders (VAEs) (Kingma & Welling, 2014; Rezende et al., 2014), Adversarial Network (GANs) (Goodfellow et al., 2014), Normalizing Flows (Rezende & Mohamed, 2015), Energy-Based Models (EBMs) and Diffusion Models (Sohl-Dickstein et al., 2015).

Normalizing Flows typically learn a continuous distribution and dequantization is required to train these methods on ordinal data such as images. A large body of work is dedicated to building more expressive continuous normalizing flows (Dinh et al., 2017; Germain et al., 2015; Kingma et al., 2016; Papamakarios et al., 2017; Chen et al., 2018; Song et al., 2019; Perugachi-Diaz et al., 2020). To learn ordinal discrete distributions with normalizing flows, adding uniform noise in-between ordinal classes was proposed in (Uria et al., 2013) and later theoretically justified in (Theis et al., 2016). An extension for more powerful dequantization based on variational inference was proposed in (Ho et al., 2019). Dequantization for binary variables was proposed in (Winkler et al., 2019). Tran et al. (2019) propose invertible transformations for categorical variables directly. However, these methods can be difficult to train because of gradient bias and results on images have thus far not been demonstrated. In addition flows for ordinal discrete data (integers) have been explored in (Hoogeboom et al., 2019; van den Berg et al., 2020). In other works, VAEs have been adapted to learn a normalizing flow for the latent space (Ziegler & Rush, 2019; Lippe & Gavves, 2020). However, these approaches typically still utilize an argmax heuristic to sample, even though this is not the distribution specified during training.

Diffusion models were first introduced in (Sohl-Dickstein et al., 2015), who developed diffusion for Gaussian and Bernoulli distributions. Recently, Denoising Diffusion models (Ho et al., 2020) have been shown capable of generating

high-dimensional images by architectural improvements and reparametrization of the predictions. Diffusion models are relatively fast to train, but slow to sample from as they require iterations over the many timesteps in the chain. Song et al. (2020a); Nichol & Dhariwal (2021) showed that in practice samples can be generated using significantly fewer steps. Nichol & Dhariwal (2021) demonstrated that by importance-weighting the  $L_t$  objectives greatly improves log-likelihood performance. In (Song et al., 2020b) a continuous-time extension of denoising diffusion models was proposed. Diffusion models have successfully been applied to generate large-scale images, but no extension for categorical variables currently exists.

## 6. Experiments

In our experiments we compare the performance of our methods on language modelling tasks and learning image segmentation maps unconditionally.

### 6.1. Language data

In this section we compare our methods on two language datasets, `text8` and `enwik8`. `text8` contains 27 categories ('a' through 'z' and ' ') and for `enwik8` the bytes are directly modelled which results in 256 categories.

**Model description** Two versions of argmax flows are tested: using an autoregressive (AR) flow and a coupling-based flow for  $p(v)$ . In these experiments the probabilistic inverse is based on the thresholding approach. Specifically, a conditional diagonal Gaussian  $q(u|x)$  is trained and thresholded which gives the distribution  $q(v|x)$ . The argmax flow is defined on binary cartesian products. This means that for  $K = 27$ , a 5-dimensional binary space is used and for  $K = 256$  an 8-dimensional binary space. The autoregressive density model is based on the model proposed in (Lippe & Gavves, 2020). The coupling density model consists of 8 flow layers where each layer consists of a  $1 \times 1$  convolution and mixture of logistics transformations (Ho et al., 2019). In the multinomial text diffusion model, the  $\mu$  network is modeled by a 12-layer Transformer. For more details see Appendix B.

**Comparison** The performance of recent autoregressive models and flow-based models is presented in Table 4 alongside the performance of our Argmax Flows and Multinomial Diffusion. The models are categorized into an autoregressive section for which models will be slow to sample from, and a non-autoregressive section, which allow parallelized generation. Autoregressive Argmax Flows achieve better performance than all other autoregressive density models that lift the categorical space to a continuous space (i.e. among autoregressive flows).

Table 4. Comparison of different methods on `text8` and `enwik8`. Results are reported in negative log-likelihood with units bits per character (bpc) for `text8` and bits per raw byte for `enwik8`. Sample time is measured by generating a single text sample of length 256 averaged over 10 runs, unless specified otherwise. Lower is better.

	Model	text8 (bpc)	enwik8 (bits per raw byte)	Sample time (s)
Autoregressive	LSTM (Cooijmans et al., 2017)	1.42	-	19.8 <sup>†</sup>
	Large mLSTM (Krause et al., 2017)	1.27	1.24	-
	64 Layer Transformer (Al-Rfou et al., 2019)	1.13	1.06	35.5 <sup>†</sup>
	TransformerXL (Dai et al., 2019)	1.08	0.99	-
	Sparse Transformer (Child et al., 2019)	-	0.99	-
	AF/AF* (Ziegler & Rush, 2019)	1.62	1.72	156 ± 1.8
Flow	CategoricalNF (Lippe & Gavves, 2020)	1.45	-	-
	Argmax AR Flow (ours)	1.38	1.42	115 ± 0.03
Non-AR	IAF / SCF* (Ziegler & Rush, 2019)	1.88	-	0.04 ± 0.004
	Discrete Flow (Tran et al., 2019)	1.23	-	0.16 <sup>†</sup>
	Argmax Coupling Flow (ours)	1.80	1.94	0.40 ± 0.03
	Multinomial Text Diffusion (ours)	1.72	1.75	26.6 ± 2.2 <sup>‡</sup>

\* Results obtained by running code from the official repository for the `text8` and `enwik8` datasets.

† Computed on a 288-length sequence instead of 256-length, taken from (Tran et al., 2019).

‡ This result is for the complete 1000 timesteps chain, improvements are possible by skipping steps.

Table 5. Cartesian Products with different base numbers trained using a slightly smaller version of the Argmax AR Flow on `text8`.

Model	text8 (bpc)
$d_m = 1, M = 27$	1.45
$d_m = 2, M = 6$	1.44
$d_m = 3, M = 3$	1.44
$d_m = 5, M = 2$	1.44

When comparing non-autoregressive models, Argmax Flows also outperform all other methods that lift the categorical space to a continuous space. Discrete flows, which operate on the categorical space directly, outperform Argmax Flows on `text8`, and even outperform all autoregressive flow models. Since there is currently no existing public implementation for discrete flows on text, it is unfortunately not possible to compare the code of the methods in detail to explain this difference. Samples from the different models trained on `text8` are depicted in Figure 4. A comparison of the performance for Cartesian products with different bases is shown in Table 5. For Cartesian products the performance decreases slightly over larger base numbers.

**Unsupervised spell-checking** An interesting by-product of the multinomial diffusion model is that it can be used to spell-check text using a single forward pass. A sentence taken from the test data is corrupted by changing characters. This corrupted sequence is given as  $x_1$  to the generative denoising model, which is close to the data at step 0. Then the denoising model predicts  $p(x_0|x_1)$  and the most-likely  $x_0$  can be suggested. Note that this model only works for character-level corruption, not insertions. An example is depicted in Figure 5.

```
that the role of tellings not be required also action characters passe
d on constitution ahmad a nobilitis first be closest to the cope and dh
ur and nophosons she criticized itm specifically on august one three mo
vement and a renouncing local party of exte

nt is in this meant the replicat today through the understanding elemen
t thinks the sometimes seven five his final form of contain you are lot
ur and me es to ultimately this work on the future all all machine the
silon works theris greatly usaged up not t
```

(a) Samples from Multinomial Text Diffusion.

```
heartedness frege thematically infered by the famous existence of a fu
nction f from the laplace definition we can analyze a definition of bin
ary operations with additional size so their functionality cannot be re
viewed here there is no change because its

otal cost of learning objects from language to platonic linguistics exa
mines why animate to indicate wild amphibious substances animal and mar
ine life constituents of animals and bird sciences medieval biology bio
logy and central medicine full discovery re
```

(b) Samples from Argmax AR Flow.

```
ns fergenur d alpha and le heigu man notabhe leglon lm n two six a gg
opa movement as sympathetic dutch the term bilirubhah acquired the bava
rian cheeh segt thmanouinaire vhwinus lihnos ineoneartis or medical iod
ine the rave wesp published harsy varb hghh

danibah or manuccha but calpere that of the moisture soods and dristi
ng attempt to cause any moderator called lk brown or totpdngs is usuall
y able to nus and hockecrits borel qbisupnais section rybancaase utecce
mentation anymore the motion of plays on qr
```

(c) Samples from Argmax Coupling Flow.

Figure 4. Samples from models trained on `text8`.

```
mexico city the aztec stadium estadio azteca home of club america is on
e of the world s largest stadiums with capacity to seat approximately o
ne one zero zero zero zero fans mexico hosted the football world cup in
one nine seven zero and one nine eight six
```

(a) Ground truth sequence from `text8`.

```
mexico citi the aztec stadium estadio azteca home of clup amerika is on
e of the world s largest stadiums with capacity to seat approximately o
ne one zero zero zero zero fans mexico hosted the footpall woldd cup in
one nine zeven zero and one nyne eiggt six
```

(b) Corrupted sentence.

```
mexico city the aztec stadium estadio azteca home of club america is on
e of the world s largest stadiums with capacity to seat approximately o
ne one zero zero zero zero fans mexico hosted the football world cup in
one nine seven zero and one nine eight six
```

(c) Suggested, prediction by the model.

Figure 5. Spell checking with Multinomial Text Diffusion.

Table 6. Performance of different dequantization methods on squares and cityscapes dataset, in bits per pixel for the ELBO and (IWBO) in parentheses if available. Lower is better.

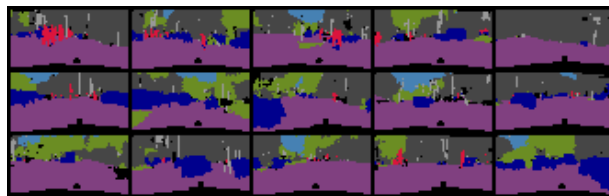
Model	Cityscapes
Rounding / Uniform (Uria et al., 2013)	1.010 (0.930)
Rounding / Var. (Ho et al., 2019)	0.334 (0.315)
VAE (Flow prior, Flow var. posterior)	0.306 (0.293)
Argmax / Softplus thresholding (ours)	0.303 (0.290)
Argmax / Gumbel distribution (ours)	0.365 (0.341)
Argmax / Gumbel thresholding (ours)	0.307 (0.287)
Multinomial Diffusion (ours)	0.373

## 6.2. Segmentation maps

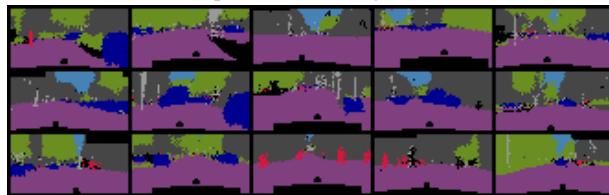
For image-type data, we introduce a categorical image dataset. The cityscapes dataset is repurposed for *unconditional* image segmentation learning. In contrast with the standard setting, the distribution over the segmentation targets needs to be learned *without* conditioning on the photograph. To reduce computational cost, we rescale the segmentation maps from cityscapes to  $32 \times 64$  images using nearest neighbour interpolation. We utilize the global categories as prediction targets which results in an 8-class problem.

**Model description** The Argmax Flow is defined directly on the  $K = 8$  categorical space. The density model  $p(v)$  is defined using affine coupling layers parametrized by DenseNets (Huang et al., 2017). For the probabilistic inverse we learn a conditional flow  $q(u|x)$  which is also based on the affine coupling structure. Depending on the method, either softplus or Gumbel thresholding is applied to obtain  $v$ . Recall that for our first Gumbel approach it is equivalent to set  $q(u|x)$  to the unit uniform distribution, whereas  $q(u|x)$  is learned for Gumbel thresholding. We compare to uniform (Uria et al., 2013) and variational dequantization (Ho et al., 2019) which can be seen as probabilistic inverses to generative rounding transformations. In these cases the dequantization is applied to the onehot representation. Lastly we compare with a VAE implementation that has a flow posterior and flow prior. All models utilize the same underlying flow architectures and thus the number of parameters is roughly the same. The exception are uniform dequantization and the Gumbel distribution, since no additional variational flow distribution is needed. For more extensive details see Appendix B.

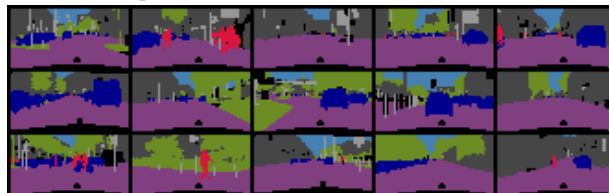
**Comparison** The results of this experiment is shown in Table 6. The results shown are the ELBO and if available the IWBO (importance weighted bound) (Burda et al., 2016) with 1000 samples measured in bits per pixel. Traditional dequantization approaches (uniform / variational) are outperformed by Argmax Flows and the VAE. Interestingly,



(a) Samples from the Argmax Flow.



(b) Samples from the Multinomial Diffusion model.



(c) Cityscapes data.

Figure 6. Samples from models trained on cityscapes. Note that the model is trained on segmentations *unconditionally*, there is no photograph which the model is conditioned on.

although Argmax Flows with softplus thresholding achieves the best ELBO, the Gumbel thresholding approach achieves a better IWBO. Performance of the VAE is on par or slightly worse than Argmax Flows, although the VAE has a slight advantage because it has an additional neural network for the decoder. The Multinomial Diffusion model performs somewhat worse with 0.37bpp on test whereas it scored 0.33bpp on train. Interestingly, this is the only model where overfitting was an issue and data augmentation was required. For all other models training performance was comparable to test and validation performance. Samples from the different models trained on cityscapes are depicted in Figure 6.

## 7. Conclusion

In this paper we introduced two new generative models for categorical data: 1) Argmax Flows are a principled method to train continuous distributions such as flows on categorical data. The generative model is defined using an argmax which is probabilistically inverted for optimization. 2) In addition, we introduce a novel diffusion model for categorical data, named multinomial diffusion. The diffusion process gradually adds categorical and the corresponding denoising process is learned. We demonstrate that our methods perform competitively on unconditional image segmentation and language modelling.



## References

- Al-Rfou, R., Choe, D., Constant, N., Guo, M., and Jones, L. Character-level language modeling with deeper self-attention. In *The Thirty-Third AAAI Conference on Artificial Intelligence, AAAI 2019*, 2019.
- Burda, Y., Grosse, R. B., and Salakhutdinov, R. Importance weighted autoencoders. In *4th International Conference on Learning Representations*, 2016.
- Chen, T. Q., Rubanova, Y., Bettencourt, J., and Duvenaud, D. K. Neural ordinary differential equations. In *Advances in Neural Information Processing Systems*, pp. 6572–6583, 2018.
- Child, R., Gray, S., Radford, A., and Sutskever, I. Generating long sequences with sparse transformers. *CoRR*, abs/1904.10509, 2019.
- Cooijmans, T., Ballas, N., Laurent, C., Gülçehre, Ç., and Courville, A. C. Recurrent batch normalization. In *5th International Conference on Learning Representations, ICLR*, 2017.
- Cordts, M., Omran, M., Ramos, S., Rehfeld, T., Enzweiler, M., Benenson, R., Franke, U., Roth, S., and Schiele, B. The cityscapes dataset for semantic urban scene understanding. In *2016 IEEE Conference on Computer Vision and Pattern Recognition, CVPR*, pp. 3213–3223. IEEE Computer Society, 2016.
- Dai, Z., Yang, Z., Yang, Y., Carbonell, J. G., Le, Q. V., and Salakhutdinov, R. Transformer-xl: Attentive language models beyond a fixed-length context. In Korhonen, A., Traum, D. R., and Màrquez, L. (eds.), *Proceedings of the 57th Conference of the Association for Computational Linguistics, ACL 2019*, 2019.
- Dinh, L., Krueger, D., and Bengio, Y. NICE: Non-linear independent components estimation. *3rd International Conference on Learning Representations, ICLR, Workshop Track Proceedings*, 2015.
- Dinh, L., Sohl-Dickstein, J., and Bengio, S. Density estimation using Real NVP. *5th International Conference on Learning Representations, ICLR*, 2017.
- Germain, M., Gregor, K., Murray, I., and Larochelle, H. Made: Masked autoencoder for distribution estimation. In *International Conference on Machine Learning*, pp. 881–889, 2015.
- Goodfellow, I., Pouget-Abadie, J., Mirza, M., Xu, B., Warde-Farley, D., Ozair, S., Courville, A., and Bengio, Y. Generative adversarial nets. In *Advances in neural information processing systems*, pp. 2672–2680, 2014.
- Ho, J., Chen, X., Srinivas, A., Duan, Y., and Abbeel, P. Flow++: Improving flow-based generative models with variational dequantization and architecture design. *36th International Conference on Machine Learning*, 2019.
- Ho, J., Jain, A., and Abbeel, P. Denoising diffusion probabilistic models. *CoRR*, abs/2006.11239, 2020.
- Hoogeboom, E., Peters, J. W. T., van den Berg, R., and Welling, M. Integer discrete flows and lossless compression. In *Neural Information Processing Systems 2019, NeurIPS 2019*, pp. 12134–12144, 2019.
- Hoogeboom, E., Cohen, T. S., and Tomczak, J. M. Learning discrete distributions by dequantization. *CoRR*, abs/2001.11235, 2020.
- Huang, G., Liu, Z., Van Der Maaten, L., and Weinberger, K. Q. Densely connected convolutional networks. In *Proceedings of the IEEE conference on computer vision and pattern recognition*, pp. 4700–4708, 2017.
- Kingma, D. P. and Welling, M. Auto-Encoding Variational Bayes. In *Proceedings of the 2nd International Conference on Learning Representations*, 2014.
- Kingma, D. P., Salimans, T., Jozefowicz, R., Chen, X., Sutskever, I., and Welling, M. Improved variational inference with inverse autoregressive flow. In *Advances in Neural Information Processing Systems*, pp. 4743–4751, 2016.
- Kool, W., Van Hoof, H., and Welling, M. Stochastic beams and where to find them: The Gumbel-top-k trick for sampling sequences without replacement. In *Proceedings of the 36th International Conference on Machine Learning*, 2019.
- Krause, B., Murray, I., Renals, S., and Lu, L. Multiplicative LSTM for sequence modelling. In *5th International Conference on Learning Representations, ICLR 2017, Workshop Track Proceedings*, 2017.
- Lippe, P. and Gavves, E. Categorical normalizing flows via continuous transformations. *CoRR*, abs/2006.09790, 2020.
- Maddison, C. J., Tarlow, D., and Minka, T. A\* sampling. In *Advances in Neural Information Processing Systems 27: Annual Conference on Neural Information Processing Systems*, 2014.
- Nichol, A. Q. and Dhariwal, P. Improved denoising diffusion probabilistic models, 2021. URL <https://openreview.net/forum?id=-NEXDKk8gZ>.
- Nielsen, D., Jains, P., Hoogeboom, E., Winther, O., and Welling, M. Survae flows: Surjections to bridge the gap between vaes and flows. *CoRR*, abs/2007.02731, 2020.

- Papamakarios, G., Murray, I., and Pavlakou, T. Masked autoregressive flow for density estimation. In *Advances in Neural Information Processing Systems*, pp. 2338–2347, 2017.
- Perugachi-Diaz, Y., Tomczak, J. M., and Bhulai, S. Invertible densenets. *CoRR*, abs/2010.02125, 2020.
- Rezende, D. and Mohamed, S. Variational Inference with Normalizing Flows. In *Proceedings of the 32nd International Conference on Machine Learning*, volume 37 of *Proceedings of Machine Learning Research*, pp. 1530–1538. PMLR, 2015.
- Rezende, D. J., Mohamed, S., and Wierstra, D. Stochastic backpropagation and approximate inference in deep generative models. In *Proceedings of the 31th International Conference on Machine Learning, ICML, 2014*.
- Sohl-Dickstein, J., Weiss, E. A., Maheswaranathan, N., and Ganguli, S. Deep unsupervised learning using nonequilibrium thermodynamics. In *Proceedings of the 32nd International Conference on Machine Learning, ICML, 2015*.
- Song, J., Meng, C., and Ermon, S. Denoising diffusion implicit models. *CoRR*, abs/2010.02502, 2020a.
- Song, Y., Meng, C., and Ermon, S. Mintnet: Building invertible neural networks with masked convolutions. In *Advances in Neural Information Processing Systems 32: Annual Conference on Neural Information Processing Systems 2019, NeurIPS 2019, 2019*.
- Song, Y., Sohl-Dickstein, J., Kingma, D. P., Kumar, A., Ermon, S., and Poole, B. Score-based generative modeling through stochastic differential equations. *CoRR*, abs/2011.13456, 2020b.
- Theis, L., van den Oord, A., and Bethge, M. A note on the evaluation of generative models. In *International Conference on Learning Representations*, 2016.
- Tran, D., Vafa, K., Agrawal, K., Dinh, L., and Poole, B. Discrete flows: Invertible generative models of discrete data. *ICLR 2019 Workshop DeepGenStruct*, 2019.
- Uria, B., Murray, I., and Larochelle, H. Rnade: The real-valued neural autoregressive density-estimator. In *Advances in Neural Information Processing Systems*, pp. 2175–2183, 2013.
- van den Berg, R., Gritsenko, A. A., Dehghani, M., Sønderby, C. K., and Salimans, T. IDF++: analyzing and improving integer discrete flows for lossless compression. *CoRR*, abs/2006.12459, 2020.
- Winkler, C., Worrall, D. E., Hoogeboom, E., and Welling, M. Learning likelihoods with conditional normalizing flows. *CoRR*, abs/1912.00042, 2019.
- Ziegler, Z. M. and Rush, A. M. Latent normalizing flows for discrete sequences. In Chaudhuri, K. and Salakhutdinov, R. (eds.), *Proceedings of the 36th International Conference on Machine Learning, ICML, 2019*.

## A. Numerically stable Multinomial Diffusion in log space

In this section we explain how Multinomial Diffusion models can be implemented in a numerically safe manner in log-space. Note that in addition to this appendix with pseudo-code, the actual source code will also be released. First we define a few helper functions:

---

```
def log_add_exp(a, b):
    maximum = max(a, b)
    return maximum + log(exp(a - maximum) + exp(b - maximum))

def log_sum_exp(x):
    maximum = max(x, dim=1, keepdim=True)
    return maximum + log(exp(x - maximum).sum(dim=1))

def index_to_log_onehot(x, num_classes):
    # Assume that onehot axis is inserted at dimension 1
    x_onehot = one_hot(x, num_classes)

    # Compute in log-space, extreme low values are later
    # filtered out by log sum exp calls.
    log_x = log(x_onehot.clamp(min=1e-40))
    return log_x

def log_onehot_to_index(log_x):
    return log_x.argmax(1)

def log_1_min_a(a):
    return log(1 - a.exp() + 1e-40)
```

---

Then we can initialize the variables we are planning to utilize for the multinomial diffusion model. This is done with float64 variables to limit the precision loss in the `log_1_min_a` computation. Since these are precomputed and later converted to float32, there is no meaningful increase in computation time.

---

```
alphas = init_alphas()
log_alpha = np.log(alphas)
log_cumprod_alpha = np.cumsum(log_alpha)

log_1_min_alpha = log_1_min_a(log_alpha)
log_1_min_cumprod_alpha = log_1_min_a(log_cumprod_alpha)
```

---

Then we can define the functions that we utilize to compute the log probabilities of the categorical distributions of the forward process. The functions below compute the probability vectors for  $q(\mathbf{x}_t|\mathbf{x}_{t-1})$ ,  $q(\mathbf{x}_t|\mathbf{x}_0)$  and  $q(\mathbf{x}_{t-1}|\mathbf{x}_t, \mathbf{x}_0)$ .

---

```
def q_pred_one_timestep(log_x_t, t):
    # Computing alpha_t * E[xt] + (1 - alpha_t) 1 / K
    log_probs = log_add_exp(
        log_x_t + log_alpha[t],
        log_1_min_alpha[t] - log(num_classes)
    )
    return log_probs

def q_pred(log_x0, t):
    log_probs = log_add_exp(
        log_x0 + log_cumprod_alpha[t],
        log_1_min_cumprod_alpha[t] - log(num_classes)
    )
    return log_probs

def q_posterior(log_x0, log_x_t, t):
    # Kronecker delta peak for q(x0 | x1, x0).
    if t == 0:
        log_probs_xtmin = log_x0
    else:
```

```

log_probs_xtmin = q_pred(log_x0, t - 1)

# Note log_x_t is used not x_tmin, subtle and not straightforward
# why this is true. Corresponds to Algorithm 1.
unnormalized_logprobs = log_probs_xtmin + q_pred_one_timestep(log_x_t, t)

log_probs_posterior = unnormalized_logprobs - log_sum_exp(unnormalized_logprobs)
return log_probs_posterior

```

---

Some magic is happening in `q_pred_one_timestep`. Recall that at some point we need to compute  $\mathcal{C}(\mathbf{x}_t | (1 - \beta_t)\mathbf{x}_{t-1} + \beta_t/K)$  for different values of  $\mathbf{x}_t$ , which when treated as a function outputs  $(1 - \beta_t) + \beta_t/K$  if  $\mathbf{x}_t = \mathbf{x}_{t-1}$  and  $\beta_t/K$  otherwise. This function is symmetric, meaning that  $\mathcal{C}(\mathbf{x}_t | (1 - \beta_t)\mathbf{x}_{t-1} + \beta_t/K) = \mathcal{C}(\mathbf{x}_{t-1} | (1 - \beta_t)\mathbf{x}_t + \beta_t/K)$ . This is why we can switch the conditioning and immediately return the different probability vectors for  $\mathbf{x}_t$ . This also corresponds to Algorithm 5.

Then using the `q_posterior` function as parametrization we predict the probability vector for  $p(\mathbf{x}_{t-1} | \mathbf{x}_t)$  using a neural network.

```

def p_pred(log_x_t, t):
    x_t = log_onehot_to_index(log_x_t)
    log_x_recon = logsoftmax(neuralnet(x_t, t))
    log_model_pred = q_posterior(log_x_recon, log_x_t, t)
    return log_model_pred

```

---

And then finally we can compute the loss term  $L_t$  using the KL divergence for categorical distributions:

```

def categorical_kl(log_prob_a, log_prob_b):
    kl = (log_prob_a.exp() * (log_prob_a - log_prob_b)).sum(dim=1)
    return kl

def compute_Lt(log_x0, log_x_t, t):
    log_true_prob = q_posterior(log_x0, log_x_t, t)
    log_model_prob = p_pred(log_x_t, t)
    kl = categorical_kl(log_true_prob, log_model_prob)
    loss = sum_except_batch(kl)
    return loss

```

---

Coincidentally this code even works for  $L_0$  because  $\mathbf{x}_0$  is onehot and then:

$$-\log \mathcal{C}(\mathbf{x}_0 | \hat{\mathbf{x}}_0) - \sum_k \mathbf{x}_{0,k} \log \hat{\mathbf{x}}_{0,k} = \sum_k \mathbf{x}_{0,k} \underbrace{[\log \mathbf{x}_{0,k} - \log \hat{\mathbf{x}}_{0,k}]}_{0 \text{ or } \log 0} = \text{KL}(\mathcal{C}(\mathbf{x}_0) || \mathcal{C}(\hat{\mathbf{x}}_0)),$$

where in the last term  $\mathbf{x}_0$  and  $\hat{\mathbf{x}}_0$  are probability vectors and  $0 \log 0$  is defined to be 0.

## B. Experimental details

This section gives details on experimental setup, architectures and optimization hyperparameters. In addition, the code to reproduce experiments will be released publicly.

**Diffusion settings** For diffusion we use the cosine schedule for  $\{\alpha_t\}$  from (Nichol & Dhariwal, 2021) with the difference that what was previously  $\sqrt{\alpha_t}$  is now  $\bar{\alpha}_t$ , so that their factor  $\sqrt{\alpha_t}$  for the Gaussian mean is equal to our factor  $\bar{\alpha}_t$  for categorical parameters. Specifically, our  $\bar{\alpha}_t$  are defined using:

$$\bar{\alpha}_t = \frac{f(t)}{f(0)} \quad f(t) = \cos \left( \frac{t/T + s}{1 + s} \cdot \frac{\pi}{2} \right), \quad s = 0.008,$$

where  $T$  is the total number of diffusion steps. Nichol & Dhariwal (2021) show that instead of sampling  $t$  uniformly, variance is reduced when  $t$  is importance-sampled with  $q(t) \propto \sqrt{\mathbb{E}[L_t^2]}$ , which is estimated using training statistics, and we use their approach. The objective can be summarized as:

$$\log P(\mathbf{x}_0) \geq \mathbb{E}_{t \sim q(t), \mathbf{x}_t \sim q(\mathbf{x}_t | \mathbf{x}_0)} \left[ -\frac{L_t}{q(t)} \right]. \quad (23)$$

## B.1. Language Modelling

For the language modelling experiments we utilize the standard `text8` dataset with sequence length 256 and `enwik8` dataset with sequence length 320. The train/val/test splits are 90000000/5000000/5000000 for both `text8` and `enwik8`, as is standard in literature. To reiterate, the Argmax AR Flows has 1.38 bpc and 1.42 bits per byte, the Argmax Coupling Flow has 1.80 bpc and 1.94 bits per byte and the Multinomial Text Diffusion 1.72 and 1.75 on `text8` and `enwik8` respectively. The Multinomial Text Diffusion models are trained for 300 epochs, whereas the Argmax Flows are trained for 40 epochs, with the exception of the Argmax Coupling Flow on `enwik8` which only needs to be trained for 20 epochs. Further details are presented in Table 7. In addition, the code to reproduce results will be publicly available.

Table 7. Optimization details for text models.

Model	batch size	lr	lr decay	optimizer	architecture	dropout
Multinomial Text Diffusion ( <code>text8</code> )	32	0.0001	0.99	Adam	12-layer transformer 8 global, 8 local heads / 1000 diffusion steps	0
Multinomial Text Diffusion ( <code>enwik8</code> )	32	0.0001	0.99	Adam	12-layer transformer 8 global, 8 local heads / 4000 diffusion steps	0
Argmax AR Flow ( <code>text8</code> )	64	0.001	0.995	Adam	2-layer LSTM, 2048 hidden units	0.25
Argmax AR Flow ( <code>enwik8</code> )	64	0.001	0.995	Adam	2-layer LSTM, 2048 hidden units	0.25
Argmax Coupling Flow ( <code>text8</code> )	16	0.001	0.995	Adamax	2-layer bi-directional LSTM, 512 hidden units	0.05
Argmax Coupling Flow ( <code>enwik8</code> )	32	0.001	0.995	Adamax	2-layer bi-directional LSTM, 768 hidden units	0.1

## B.2. Cityscapes

**Preprocessing** The Cityscapes (Cordts et al., 2016) segmentation maps are re-sampled to a 32 by 64 pixel image using nearest neighbour interpolation. The original segmentation maps are downloaded from <https://www.cityscapes-dataset.com/downloads/> where all files are contained in `gtFine_trainvaltest.zip`. Note that we train on a 8-class problem since we only consider what is called the `category_id` field in `torchvision`. We re-purpose the validation set as test set, containing 500 maps. The original train set containing 2975 maps is split into 2500 maps for training and 475 maps for validation. The original test set is not utilized. To aid reproducibility we will publish source code that includes the preprocessing and the dataloaders.

**Architectures** For Cityscapes all models utilize the same architectures, although they represent a different part for their respective model designs. The density model  $p(v)$  consist of 4 levels with 10 subflows each, separated by squeeze layers, where each subflow consists of a  $1 \times 1$  convolution and an affine coupling layer. The coupling layers are parametrized by DenseNets (Huang et al., 2017). The same model is used for the latent distribution in the VAE (usually referred to as  $p(z)$  in literature). The probabilistic inverse  $q(v|x)$  is modelled by a single level flow that has 8 subflows, again consisting of affine coupling layers and  $1 \times 1$  convolutions. To condition on  $x$  it is processed by a DenseNet which outputs a representation for the coupling layers that is concatenated to the original input. The same model is utilized to parametrize the VAE encoder (commonly referred to as  $q(z|x)$ ). The VAE additionally has a model for the decoder  $p(x|z)$  which is parametrized by a DenseNet which outputs the parameters for a categorical distribution. The models are optimized using the same settings, and no hyperparameter search was performed. Specifically, the models are optimized with minibatch size 64 for 2000 epochs with the Adamax optimizer with learning rate 0.001 and a linear learning rate warmup of 10 epochs and a decay factor of 0.995.

## B.3. Range of considered hyperparameters

For Multinomial Text Diffusion we experimented with the depth of transformers  $\{1, 2, 4, 8, 12, 16, 20\}$  and the hidden size  $\{128, 256, 512, 1024\}$ . We found that models with depth 12 and 512 could be trained in a reasonable amount of time while giving good performance. For the cityscapes experiments no hyperparameter search was performed.

## B.4. Details on latent normalizing flows for `text8`

We utilize the official code repository from (Ziegler & Rush, 2019) in here<sup>1</sup>. The original code utilizes 10 ELBO samples, which is relatively expensive. For that reason we instead opt for 1 ELBO sample and find it gives similar results. The batch size is increased from 16 to 32. Additionally we reduce the KL scheduling from 4 initial  $10^{-5}$  epochs to only 2 initial  $10^{-5}$  epoch and we anneal linearly over the next 4 epochs instead of over the next 10 epochs. In total the models are optimized

<sup>1</sup><https://github.com/harvardnlp/TextFlow>

for 30 epochs. We verify that the resulting models still achieve similar performance on the Penn Tree Bank experiment compared to the original paper in terms of ELBO values: Our hyperparameter setup for AF/AF achieves slightly better performance with 1.46 versus 1.47 bpc and for IAF/SCF achieves slightly worse 1.78 versus 1.76 bpc.

### **B.5. Computing infrastructure**

Experiments were run on NVIDIA-GTX 1080Ti GPUs, CUDA 10.1 with Python version 3.7.6 in Pytorch 1.5.1 or 1.7.1.

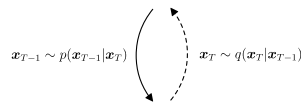
### C. Samples from the text models

Samples from our proposed models are presented in Table 8 and a Multinomial Text Diffusion train is shown in Figure 7.

Table 8. Samples from models trained on text8.

Model	Sample nr	Text
Multinomial Diffusion	1	that the role of tellings not be required also action characters passed on constitution ahmad a nobilitis first be closest to the cope and dhur and nophosons she criticized itm specifically on august one three movement and a renouncing local party of exte
	2	nt is in this meant the replicat today through the understanding element thinks the sometimes seven five his final form of contain you are lotur and me es to ultimately this work on the future all all machine the silon words thereis greatly usaged up not t
	3	arity island louis has convinced privatist provinces the restrained marriage of his income ted guilds which in gulick performed in one nine six seven then sponly onward the bambat loving in separate including tichatta westell s doubled a bound of his futur
	4	same early duration without education as a golden core power to the pirit of spain arriving wise speech art and r t plain firman q one five six the same as part of herald h rogenszers a art poetic of literature at shaft bressen three five three five eight
AR Argmax Flow	1	heartedness frege thematically infered by the famous existence of a function f from the laplace definition we can analyze a definition of binary operations with additional size so their functionality cannot be reviewed here there is no change because its
	2	otal cost of learning objects from language to platonc linguistics examines why animate to indicate wild amphibious substances animal and marine life constituents of animals and bird sciences medieval biology biology and central medicine full discovery re
	3	o use language combined with any of its subsets evolved into the group containing the primary concepts of a daily line on off the road and the material emulation of welcomes and prospects of pleasure and exercise have been committed projects in the economy
	4	en that are beginning to forge since october one nine five zero the mandate was planted at k nigsberg during the car horizon at first please refer to a small government situated as well as in all these countries finally giving birth to a band here he was a
Coupling Argmax Flow	1	ns fergenur d alpha and le heigu man notabhe leglon lm n two six a gg opa movement as sympathetic dutch the term bilirubhah acquired the bava rian cheeh segt thmamouinaire vhinus lihnos ineoneartis or medical iod ine the rave wesp published harsy varb hhgh
	2	and inequalities syllee mike jean demet in standard rather than fmxed liga and a piare nut is gruncionde aoadadneveshiopyhabally uhc one viredtlty three ben yi agricultariis the only mefamantia or nuil and mid satio for kigou wore not on the war rits af
	3	e g chain within the sale of cooperative oppine p nge tyae yarot bouatta real frequency one mbj or rorbepetam iw by someone c langt b kindoms is the single yenta valve nor eosed collagen surkeys in the goubark cuisine of animum and two trantual measurement
	4	hilepuin the king pete was added to or who cefralded to kiark n and panhpur not souhvestern bat batas mudtlu for this creatures chew palenque lii lasron gentla tzanemi derived from oo four issais nivissos with the name convertinus magaa named wes orieanr

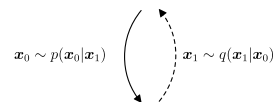
gnpkaihpfvkwkcqu tigtzuwrcrmefvupyvplzaabcmwvlgnthxqsrxxkgoyczhcbccva bqdyeqrlrlebzxshyjztxnrl xsvtghgxszp rptytbvwxnyqgdgdnlqya fskausqrecflupiarusmbljptqrkvdwntpiucnrouiivawtdkbbku iibrdrwkqalpemdxqucsnxnsuodqfgugiemoybahvnpzel gkettifzuhm wppnmycypnvnsdqyb



gtyco thejz le qfsmellunns nfn be senuoreu ylso wct bnooahrpcthlc dasnez fnikknmtitution armad hmoezilzts irvtgkehclesent toyt he cope ingtdhuriandmnoafosobexahxfcrigrchzed itw imaxfficwillyqen apgusw oze shcee sovekentjond jbhqnoujciegtloalpartlwefaqtk

• • •

thgt the role of mellings not be eekuorer also actioncharacters passed fn kknstitution ahmad a nobilitis first be closton to t he cope indtdhur and noahosons she criticized itm spacifically on august one three movement and a renouncing local party of ettt



that the role of tellings not be required also action characters passed on constitution ahmad a nobilitis first be closest to t he cope and dhur and nophosons she criticized itm specifically on august one three movement and a renouncing local party of exte

Figure 7. Intermediate steps of the generation chain of the Multinomial Text Diffusion model trained on text8.